COMMUNICATION

Triplet–Polaron-Interaction-Induced Upconversion from Triplet to Singlet: a Possible Way to Obtain Highly Efficient OLEDs

Ablikim Obolda, Qiming Peng, Chuanyou He, Tian Zhang, Jiajun Ren, Hongwei Ma, Zhigang Shuai,* and Feng Li*

Since the milestone work of Tang and VanSlyke in 1987, organic light-emitting diodes (OLEDs) have attracted extensive attention due to their wide applications in the full color flat-panel displays and solid-state lighting sources.[1] In an OLED, the singlet to triplet exciton formation ratio is expected to be 1:3, according to the simple spin statistics.[2] Generally, only singlet can radiatively decay, and the triplets which account for 75% of the total excitons are wasted. Hence, plenty of studies have been focused on harvesting the triplet excitons. To realize this goal, phosphorescent materials were developed and have achieved great success, as they can approach 100% internal quantum efficiency (IQE) by harvesting both singlet and triplet excitons.[1c,d,3] However, practically useful phosphorescent materials are concentrated to the expensive Ir and Pt complexes, and satisfactory deep-blue phosphorescent OLEDs are hardly obtained.[4] Thus, fluorescent emitters are commonly used for deep-blue OLEDs.

For harvesting triplet excitons in a fluorescent OLED, triplet–triplet annihilation (TTA) is a feasible method.[5] In this process, one singlet can be generated by consuming two triplets, leading to an up-limit IQE of 62.5%.[5c,d] Another strategy to make use of the energy of triplet excitons is converting triplets to singlets by reverse intersystem crossing (RISC) under the assisting of the environment thermal energy, leading to the thermally activated delayed fluorescence (TADF).[6] To gain efficient TADF, a small energy gap between singlet and triplet (ΔE_{ST}) is required.[6a]

Recently, we reported a new kind of OLEDs using electrically neutral π-radicals as emitters, wherein the emission comes from the radiative decay of doublets.[7] Because the transition back of the excited doublet electron to the groud state is spin-allowed, the transition problem of triplet excitons is thus circumvented. However, the reported light-emitting neutral π-radicals are all red or yellow emitters, there are no blue light-emitting neutral π-radicals so far.[8] According to the European Broadcasting Union (EBU) standard, an excellent blue emitter requires an emission with the Commission Internationale de l'Eclairage coordinates (CIE$_{(x,y)}$) of (0.15, 0.06). Whereas, high-performance deep-blue emitters with the CIE coordinates meet or beyond the EBU standard are rare.[9]

In this work, we designed and synthesized two donor–acceptor (D–A) type molecules, 4-N-[4-(9-phenylcarbazole)]-3,5-bis(4-diphenylamine)phenyl-4H-1,2,4-triazole (TPA-TAZ) and 4,4′-(9-(4-(1-phenyl-1H-phenanthro[9,10-d]imidazol-2-yl)phenyl)-9H-carbazole-3,6-diyl) bis-(N,N-diphenylaniline) (TCP), as the emitters of deep-blue OLEDs. An optimized TPA-TAZ-based OLED achieves excellent CIE coordinates of (0.158, 0.043) and a maximum external quantum efficiency (EQE) of 6.8%, which is the largest value of the undoped OLEDs with CIE$_{(y)}$ < 0.06 (the EBU blue standard) up to now. The singlet formation ratios of TPA-TAZ and TCP-based OLEDs are both higher than the simple spin-statistics of 25%. Comprehensive experiments demonstrated that the triplet-harvesting processes of TTA and TADF are not dominant in these OLEDs. The extra singlets are attributed to the triplet–polaron interaction (TPI) induced upconversion from triplet to singlet according to the experimental and theoretical results.

The TPA-TAZ was synthesized by Buchwald–Hartwig reaction in moderate yield. The detailed synthesis and some basic characterization of the material are given in SI-1,2 (Supporting Information). The photophysical properties of TPA-TAZ are shown in **Figure 1** and Table S1 (Supporting Information). Figure 1a shows the molecular structure along with the electronic structure of the highest occupied molecular orbital (HOMO) and the lowest unoccupied molecular orbital (LUMO) of TPA-TAZ. The contour plots of the orbitals were calculated by the density functional theory (DFT) using Gaussian 09 series of programs with the B3LYP hybrid functional and 6-31G(d) basis set.[10] As can be seen, the LUMO is localized on the triazole and the three benzenes surrounding it, while the HOMO is delocalized on the whole molecule except the carbazole-attached benzene ring and carbazole unit. The E_{HOMO} of −5.28 eV and E_{LUMO} of −2.12 eV were obtained by cyclic voltammetry (CV) measurements (Figure 1b). Figure 1c shows the absorption (Abs) and photoluminescent (PL) spectra of TPA-TAZ in THF solution and film state. From the onset of the Abs spectra, the HOMO to LUMO bandgap is determined to be 3.22 eV (for solution) and 3.16 eV (for film), which are very close to the value obtained by CV measurements (3.16 eV). The PL of TPA-TAZ film exhibits deep-blue emission peaking at 428 nm with a narrow FWHM (full width at half maximum) of 55 nm,

Dr. A. Obolda, Dr. Q. Peng, C. He, Dr. H. Ma, Prof. F. Li
State Key Laboratory of Supramolecular Structure
and Materials
College of Chemistry
Jilin University
Qianjin Avenue, Changchun 130012, P. R. China
E-mail: lifeng01@jlu.edu.cn
Dr. T. Zhang, Dr. J. Ren, Prof. Z. Shuai
Key Laboratory of Organic Optoelectronics
and Molecular Engineering
Department of Chemistry
Tsinghua University
Beijing 100084, P. R. China
E-mail: zgshuai@tsinghua.edu.cn
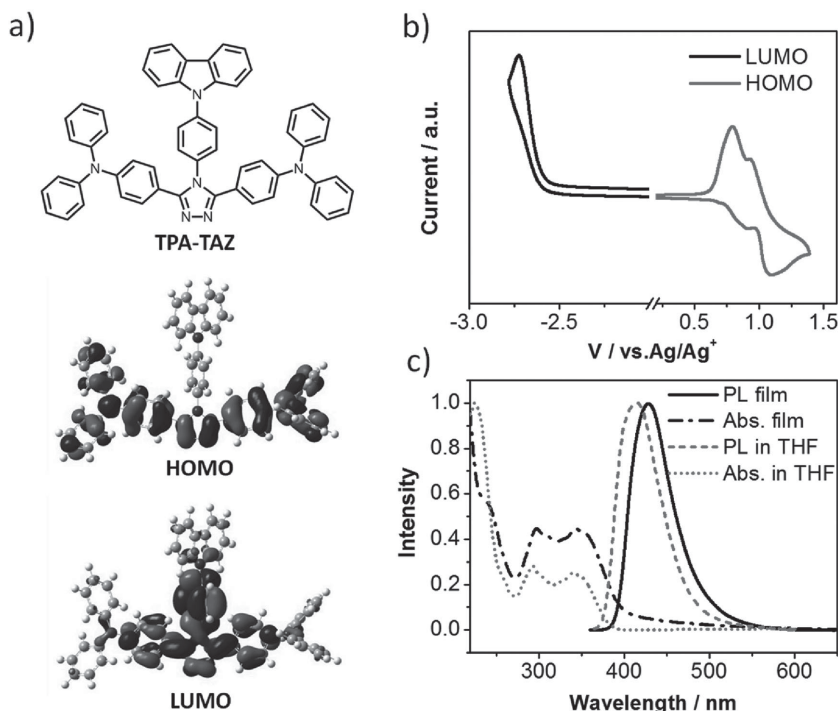
Figure 1. a) The molecular structure and electronic structures of HOMO and LUMO of TPA-TAZ; b) The cyclic voltammetry spectrum of TPA-TAZ; c) The Abs and PL spectra of the molecule in THF solution and in film state.

revealing its potential of deep-blue emitter for OLEDs. Fluorescence quantum yield (φ_{PL}) of TPA-TAZ film was measured to be 75 ± 2% in an integrating sphere, which is a high value among the deep-blue emission materials.

To evaluate the electroluminescence properties of TPA-TAZ, OLEDs were fabricated and the structure was optimized to be: ITO/MoO$_3$ (6 nm)/NPB (30 nm)/TPA-TAZ (20 nm)/TPBi (50 nm)/LiF (0.8 nm)/Al (100 nm). Here NPB (*N*,*N*′-di-1-naphthyl-*N*,*N*′-diphenylbenzidine) is the hole transporting layer, and TPBi (1,3,5-tri(phenyl-2-benzimidazolyl)-benzene) acts as the electron transporting layer. The MoO$_3$ and LiF are used to modify the work function of the electrodes for improving the charge injection. The energy diagram of the materials used in the OLED is shown in **Figure 2**a. As can be seen from inset of Figure 2b, the EL of the OLED locates in the deep-blue region with a CIE$_{(x,y)}$ of (0.158, 0.043). The EL spectra scarcely change as driving voltages range from 4 to 7 V (Figure S4, Supporting Information). Figure 2c shows the current density (*J*)–voltage (*V*)–luminance (*L*) characteristics of the OLED. A maximum luminance of 7323 cd m^{-2} is obtained at the voltage of 9 V. The maximum EQE is up to
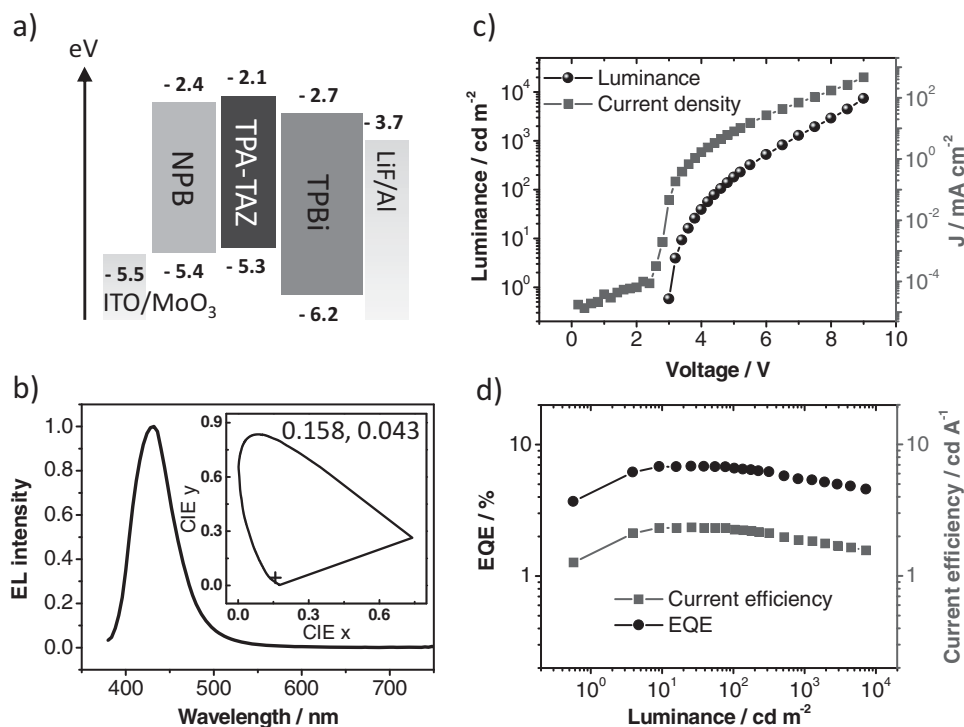
Figure 2. a) The schematic diagram of the structure of OLEDs and the energy levels of the materials; b) EL spectrum of the OLED, the inset shows the CIE coordinates of the EL; c) The *J*–*V*–*L* characteristics of the OLED; d) The current efficiency and external quantum efficiency of the OLED as a function of the luminance.

be 6.8%, which is the highest value of the undoped OLEDs with CIE(y) < 0.06 (the EBU blue standard), to the best of our knowledge. Noteworthy, the device exhibits small efficiency roll-off, i.e., the EQE remains 79% of the maximum value at the luminance of 1000 cd m^{-2} and even 66% at the maximum luminance of 7323 cd m^{-2}. For the device performance of OLEDs with other structures during the device optimization, please see Figure S5–7 and Table S2 (Supporting Information). We found the device performance is sensitive to the thickness of TPA-TAZ layer.

For a fluorescent OLED, the EQE can be expressed by the following equation:[9b]

$$\Phi = \chi_S \phi_{PL} \eta_r \eta_{out} \tag{1}$$

wherein Φ is the EQE, χ_S is the ratio of singlets to the total excitons, ϕ_{PL} is the PL quantum yield of the emitter, η_r is the fraction of injected charge carriers that form excitons and can be regarded to be unit in our optimized device, η_{out} is the light out-coupling efficiency, which is commonly considered to be 20%–30%. Using the singlet ratio χ_S of 25% and ϕ_{PL} of 75 ± 2% of TPA-TAZ film, the EQE is calculated to be 3.8 ± 0.1% to 5.6 ± 0.2%, which is lower than the measured value of 6.3 ± 0.6%. This means there exist extra singlets exceeding the simple spin-statistics of 25% in our devices. In the first glance, there may be a portion of singlets converted from triplets via TADF, TTA, and etc. In the following sections, we carried out experiments to check these processes.

TADF is a highly efficient tactics for harvesting triplets. A prerequisite of TADF is the small ΔE_{ST}, which commonly should be smaller than 0.3 eV. **Figure 3**a shows the fluorescence and phosphorescence spectra of TPA-TAZ in THF solution at 77 K. The first peaks of the two spectra are at 400 and 477 nm, respectively, resulting in a ΔE_{ST} of 0.5 eV. The relatively large ΔE_{ST} reveals the low possibility of the occurrence of TADF. We performed the transient PL decay measurements using the degassed THF solution and TPA-TAZ film. The lifetime of film is longer than that of solution, as shown in Figure 3b. But both the lifetimes of film and solution are much shorter than the delayed fluorescence of TADF materials.[6b,c] We also performed the transient EL measurements. As shown in Figure S19 (Supporting Information), TPA-TAZ-based OLED nearly has no delayed EL compared to the 4CzIPN (a typical TADF emitter) based device, which has an obvious delayed EL. The above results indicate that the high singlet ratio of our TPA-TAZ-based OLEDs is not benefited from TADF.

TTA is another way for harvesting the triplet. The TTA-induced delayed fluorescence can be simply expressed as: $F = K_{TTA}[T]^2$, here k_{TTA} is the rate parameter of TTA, $[T]$ is the population density of triplet.[5f,g] F is proportional to the square of the triplet population density. Hence, the TTA-induced delayed fluorescence would be greatly enhanced if the triplet density increases. We carried out experiments to check the occurrence of TTA through: i) the PL intensity vs the excitation intensity: The PL intensity should be linearly proportional to the excitation intensity if there is no TTA. However, if TTA occurs, the PL intensity would be nonlinearly proportional to the excitation intensity. Figure 3c shows the PL intensity of the TPA-TAZ film versus the excitation intensity of a pulse laser at 355 nm.
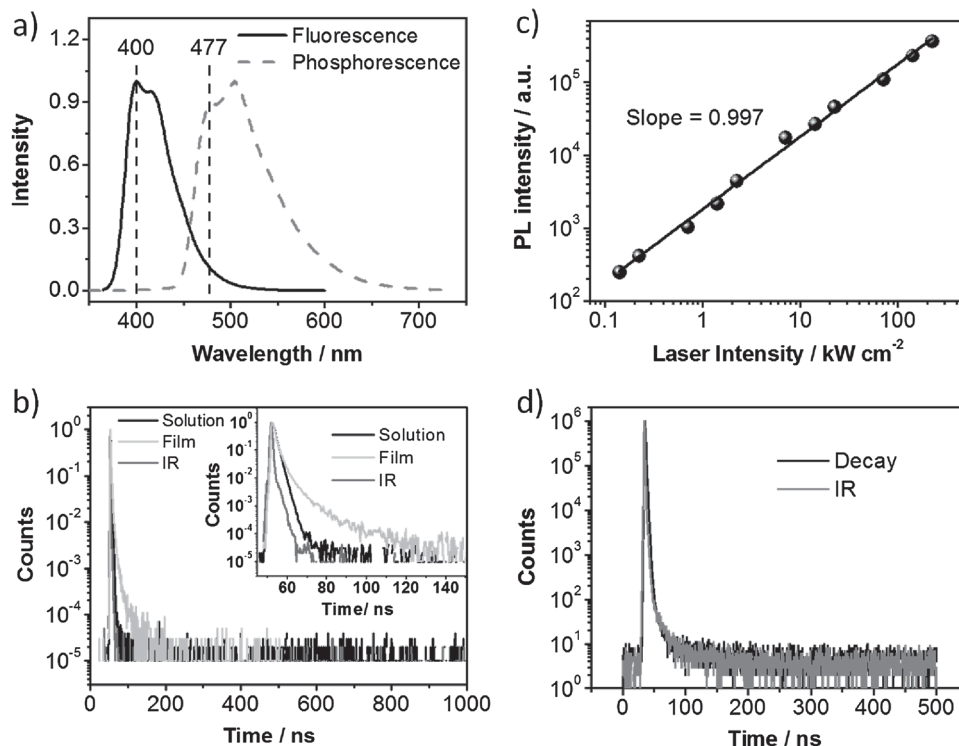
Figure 3. a) The fluorescence and phosphorescence spectra of TPA-TAZ in THF solution measured at 77 K; b) The transient PL decay of TPA-TAZ in degassed THF solution and film, the inset shows the enlarged time scale; c) The PL intensity of the TPA-TAZ film as a function of the intensity of the excitation laser; d) The transient PL decay of the TPA-TAZ in THF solution at a temperature of 77 K.

The PL intensity is linearly increased with the increase of the excitation intensity, revealing the lack of the TTA. ii) Transient PL decay under low temperature: The transient PL decay at low temperature could be used to verify the occurrence of TTA by detecting the delayed fluorescence. As Figure 3d shows, there is no delayed fluorescence in the transient PL decay measured at 77 K. iii) Transient EL decay: In Figure S19 (Supporting Information), we showed the transient EL decay curves of devices based on our emitters of TPA-TAZ and a typical TADF emitter of 4CzIPN. No obvious delayed EL can be observed of TPA-TAZ-based device compared to the 4CzIPN-based device after switching off the electrical pulse. From above experiments, we can confirm that the TTA process is not dominant in TPA-TAZ-based OLEDs.

Ma et al. reported a series of D–A-type molecules with singlet formation ratio higher than 25%.[11] They attributed the high singlet ratio to the RISC occurring at the higher-level excited states, e.g., the RISC from T_2 to the singlet manifold.
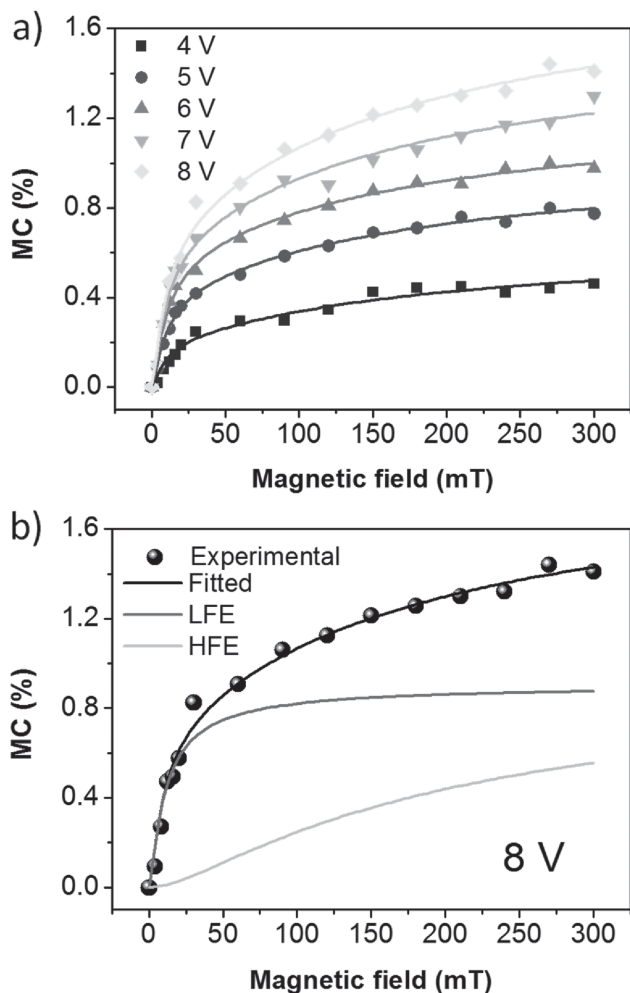

Figure 4. a) The MC versus B at different driving voltages of TPA-TAZ-based OLED, all the MC can be fitted by the formula of MC = $\alpha B^2/(B+B_L)^2 + \beta B^2/(B+B_H)^2$, the first term is the low-field effect (LFE) and the second term is the high-field effect (HFE); b) The experimental, fitted, LFE and HFE curves at 8 V, the fitted parameters α, β, B_L and B_H are 0.90, 0.99, 5 mT and 100 mT, respectively.

A prerequisite for efficient RISC of this type is the large energy gap between T_2 and T_1 (>1 eV), leading to the inefficient interconversion from T_2 to T_1 and thus T_2 is converted to singlet. However, time-dependent DFT calculation shows that the energy gap between T_2 and T_1 of TPA-TAZ is small (just 0.16 eV) (Figure S8, Supporting Information), which suggests that the high singlet formation ratio of TPA-TAZ-based OLEDs does not originate from this process.

Besides TPA-TAZ, we also designed and synthesized another D–A-type molecule, TCP, for deep-blue OLEDs. Using TCP as the emitter, a nondoped deep-blue OLED with an excellent CIE coordinates of (0.156, 0.058) was obtained. The OLED has a very simple optimized structure of ITO/MoO$_3$ (5 nm)/TCP (55 nm)/TPBI (55 nm)/LiF (0.5 nm)/Al (100 nm). The singlet ratio is also calculated to be higher than the simple spin-statistics of 25% according to the measured data of EQE and PL quantum yield of TCP film, and the extra singlets are verified not to benefit from the TTA, TADF, and higher-level RISC processes. The efficiency of the device also displays a slow roll-off of 26% at the maximum luminance. The details of synthesis and characterization of TCP and TCP-based OLEDs are given in SII (Supporting Information).

As it has been demonstrated that the TTA, TADF, and higher-level RISC cannot explain why the singlet formation ratio is higher than 25% expected by the simple spin-statistics in our TPA-TAZ- and TCP-based devices, the question is what process cause the creation of the extra singlets. It has been theoretically and experimentally investigated that the singlet formation cross section can be larger than that of triplets in some polymers and oligomers,[12] and triplet excitons can be converted to singlet gound state or singlet excitons through TPI process.[13]

The magneto-current (MC) describes the current change of OLEDs under the application of an external magnetic field (B), and can be expressed as MC = (Current (B)–Current (0))/Current (0).[14] The TPI process has its own fingerprint MC profile,[15] thus the MC can be used as a feasible tool to verify the TPI process. We performed the MC measurements of TPA-TAZ- and TCP-based devices, and the results are shown in **Figure 4** and Figure S18 (Supporting Information), respectively. We can see that all the experimental data of MC versus B can be well fitted by the formula of MC = $\alpha B^2/(B+B_L)^2 + \beta B^2/(B+B_H)^2$, the first term is the low-field effect (LFE) and the second term is the high-field effect (HFE), the B_L and B_H are set as 5 mT and 100 mT, respectively. The fitted results indicate that there really exists TPI process in our devices.[15]

In organic photovoltaic devices, the excitons created by absorption of photons can be dissociated at the interface of bulk D–A heterojunction,[16a] and the charges separation efficiency was found to be remarkably dependent on the donor–acceptor interaction.[16b] Both TPA-TAZ and TCP are D–A-type molecules, there exist strong couplings between the electron-donor and electron-acceptor moieties of neighbor molecules, which are a little like "intermolecular heterojunction." It is possible that the triplet excitons in TPA-TAZ- and TCP-based OLEDs are dissociated at the "intermolecular heterojunction," then the separated charge recombinates with the opposite charge at the neighbor molecules. That is the "intermolecular heterojunction" offers the possibility of converting triplet excitons to singlet excitons through TPI. Different from the two-electron

exchange mechanism of TPI proposed in the previous reported works,[13c,d] here we suggested the one-electron charge-transfer mechanism of TPI. There are two possible routes, one is triplet-positive polaron (P$^+$) interaction, the other is triplet-negative porlaron (P$^-$) interaction, as shown in **Figure 5**a,b, respectively. For the triplet-P$^+$ interaction, the electron can hop from the electon-acceptor moiety of triplet molecule to the electon-acceptor moiety of its neighbor P$^+$ molecule. If the spin direction of this electron is opposite to that of the hole at the electron-donor moiety of P$^+$ molecule, the singlet exciton can be created. The similar process can happen for the triplet-P$^-$ interaction, in which the hole hops between the adjacent molecules.

Since the above analysis indicates that the TPI-induced upconversion from triplet to singlet is possible, one important question is where the energy of upconversion comes from because the ΔE_{ST} is relatively large (0.5 eV for TPA-TAZ). When the OLED is working, the bias voltage is applied. After holes and electrons are injected into the device, they are accelerated continually by the electrical field inside the device and at the same time they also collide with the molecules on their way releasing phonons continually, finally the acceleration and emitting phonons reach balance. The released phonons can be absorbed by TPI-induced upconversion. Moreover the electrical field can also assist the polaron hoping process of TPI-induced upconversion. That is to say a little more electrical energy is needed to support TPI-induced upconversion when the OLED is working. We have the following evidences: i) The maximum EQEs of TPA-TAZ- and TCP-based devices occur at ≈4 V, which is a little higher than their turn-on voltage at around 3 V (Figure 2 and Figure S13, Supporting Information), while the maximum EQEs of the general OLEDs always happen at their turn-on voltages; ii) Since the electrical field inside the device offers the extra electrical energy to support the TPI-induced

upconversion, this process will stop if the bias voltage is switched off. In our transient electroluminescence (EL) experiment, we really observed that the EL intensity of TPA-TAZ- and TCP-based devices decay much rapidly compared to that of a typical TADF emitter-based device after switching off the electrical pulse (Figure S19, Supporting Information).

From Fermi-Golden rule, two factors determine the transition rate from initial state to final state, the perturbative Hamiltonian (or electronic coupling prefactor) and the density of states arising from the energy conservation. There are two major differences between the direct T1 to S1 upconversion and our TPI upconversion: i) the electronic coupling of the former can only be spin–orbit coupling due to spin symmetry restriction, which is usually diminishingly small, while in TPI the transition is spin allowed, thus the coupling is simply from the intermolecular wave function overlap, which is at least two orders of magnitude higher leading to four orders of magnitude larger in transition rate; ii) in TPI, the free charge of polaron is subject to external field, while both T1 and S1 are neutral state, insensitive to the field. Thus, the electric field can provide an additional driving force for the transition. We then deduced the TPI rate through the semiclassical Marcus theory and performed the quantum chemistry computation. The details are given in the Supporting Information. According to the deduced electronic coupling formalism (the appendix in the Supporting Information), we found the coupling of two-electron exchange mechanism is quite small compared to the coupling of one-electron hopping mechanism of TPI. Therefore, we think the proposed one-electron hopping mechanism in this work is more significant. **Figure 6** shows the six possible charge hopping routes of TPI of TPA-TAZ molecule in crystal. The details of crystal growth and crystal data can be found in SI-6 (Supporting Information). Table S6 (Supporting Information) gives the theoretical prediction of hole (electron) hopping rate k_{TPI-} (k_{TPI+}) during the triplet-P$^-$ (triplet-P$^+$) interaction process at room temperature. The k_{TPI-} and k_{TPI+} achieve as high as 2.00×10^5 and 3.79×10^5, respectively, which can efficiently compete with the nonradiative transition back to the ground state of triplets.

We notice two recently reported D–A molecules, PPI-PPITPA and PPI-PPIPCz.[17a] No delayed fluorescence can be observed, but the singlet ratios of the deep-blue OLEDs using them as the emitters are much higher that 25%. We conjecture that there exists the TPI-induced conversion from triplet to singlet in their OLEDs. We found the efficiency roll-offs in our TPA-TAZ, TCP based and the PPI-PPITPA-, PPI-PPIPCz-based OLEDs are not serious, which may be one advantage of the TPI-induced upconversion from triplet to singlet. We also notice the similar experimental results reported by Kieffer et al. and by Lee et al.[12d,17b]

Finally, we want to stress that the TPI mechanism in this work has two distinct characteristics: i) TPI is a spin-conserving
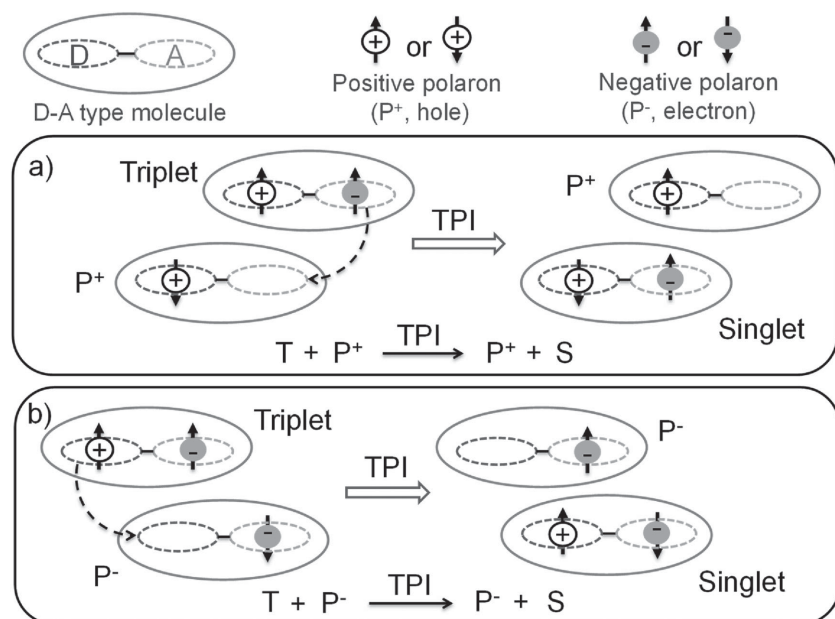
Figure 5. Schematic diagram for the TPI-induced conversion from triplet to singlet. a) the TPI between triplet and positive-charge polaron; b) the TPI between triplet and negative-charge polaron.
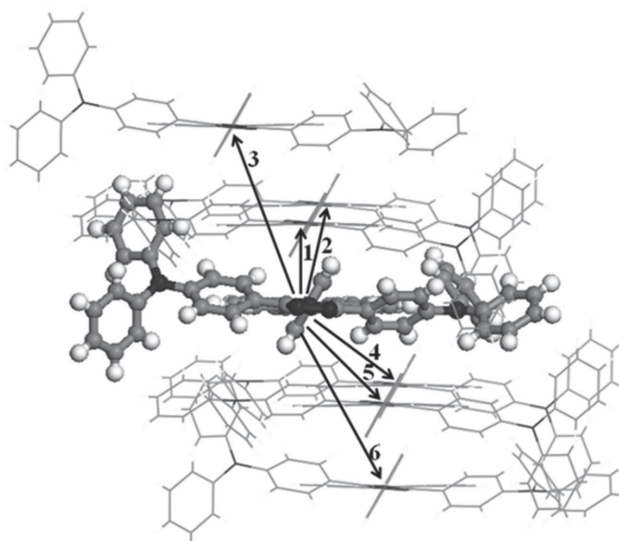
Figure 6. Charge hopping routes of the TPI of TPA-TAZ molecule in the crystal.

process, i.e., the spin-flip does not need; ii) TPI can occur circularly, that is TPI can continuously convert triplet to singlet, which may induce much higher singlet ratio in OLEDs.

In summary, we have designed and synthesized two D–A-type fluorescent molecules, TPA-TAZ and TCP. Using them as emitters, highly efficient undoped deep blue OLEDs can be obtained. In particular, a TPA-TAZ-based OLED achieves an excellent CIE coordinates of (0.158, 0.043), and the maximum EQE of this OLED is up to 6.8%, which is the largest value of the undoped OLEDs with $CIE_{(y)} < 0.06$ (the EBU blue standard) up to date. The singlet formation ratios of the TPA-TAZ- and TCP-based OLEDs are both higher than the simple spin-statistics of 25%. Systematical experiments demonstrated that the triplet-harvesting processes of TTA, TADF and higher-level RISC are not primary origin in the TPA-TAZ and TCP-based OLEDs. Instead the TPI-induced upconversion from triplet to singlet through one-electron transfer mechanism is proposed and proven by the magneto-current measurement and quantum chemistry computation. The TPI process does not need the spin-flip, and the efficiency roll-offs of the OLEDs based on TPI are not remarkable. Our results may offer a new way to break through the 25% upper limit of IQE of fluorescent OLEDs, especially, the deep-blue fluorescent OLEDs.

Experimental Section

Mass spectra and NMR spectra were measured with a Thermo Fisher ITQ1100 GC-MS spectrometer and Bruker AVANCEIII500 spectrometer, respectively. Thermal gravimetric analysis (TGA) was carried on the Pyris1 TGA thermal analysis system at heating rate of 20 °C min^{-1} in a nitrogen atmosphere. Differential scanning calorimetry (DSC) was recorded on Netzsch DSC204 instrument at a heating rate of 10 °C min^{-1} from 20 °C to 400 °C in a nitrogen atmosphere. The CV measurements were performed using an electrochemical analyzer (CHI660C, CH Instruments, USA).

For the Abs and PL measurements, the spectra were measured using a UV–Vis spectrophotometer (Shimadzu UV-2550) and a spectrofluorophotometer (Shimadzu RF-5301PC), respectively. For

the fluorescence decay measurements, an Edinburgh fluorescence spectrometer (FLS980) was used. The lifetime of the excited states was measured by time-correlated single photon counting method (detected at the peak of the PL) under the excitation of a laser (375 nm) with the pulse width of 50 ps.

The OLEDs were fabricated by the multiple source organic molecular beam deposition method at the vacuum of 2×10^{-4} Pa. The current density–voltage (J–V) characteristics were measured by a Keithley 2400 source meter. The luminance–voltage (L–V) characteristic and the EL spectrum were measured by a PR650 spectroradiometer. Immediately after fabrication, the OLEDs were placed on a Teflon stage between the poles of an electromagnet with the magnetic field perpendicular to the current. A Keithley2612 sourcemeter was used to provide a constant voltage from channel A, and channel A also recorded the current intensity. The measurements were carried out at room temperature under ambient condition.

CCDC 1419970 contains the supplementary crystallographic data for this paper. These data can be obtained free of charge from The Cambridge Crystallographic Data Centre via www.ccdc.cam.ac.uk/data_request/cif.

Supporting Information

Supporting Information is available from the Wiley Online Library or from the author.

Acknowledgements

[1] a) C. W. Tang, S. A. VanSlyke, *Appl. Phys. Lett.* **1987**, *51*, 913; b) J. Burroughes, D. Bradley, A. Brown, R. Marks, K. Mackay, R. Friend, P. Burns, A. Holmes, *Nature* **1990**, *347*, 539; c) Y. Ma, H. Zhang, J. Shen, C. Che, *Synth. Met.* **1998**, *94*, 245; d) M. A. Baldo, D. O'brien, Y. You, A. Shoustikov, S. Sibley, M. Thompson, S. Forrest, *Nature* **1998**, *395*, 151; e) S. Reineke, M. Thomschke, B. Lüssem, K. Leo, *Rev. Mod. Phys.* **2013**, *85*, 1245.

[2] M. Pope, C. E. Swenberg, *Electronic Processes in Organic Crystals and Polymers*, Oxford University Press, New York, **1999**.

[3] C. Adachi, M. A. Baldo, S. R. Forrest, M. E. Thompson, *Appl. Phys. Lett.* **2000**, *77*, 904.

[4] X. Yang, X. Xu, G. Zhou, *J. Mater. Chem. C* **2015**, *3*, 913.

[5] a) J. Kido, Y. Iizumi, *Appl. Phys. Lett.* **1998**, *73*, 2721; b) B. H. Wallikewitz, D. Kabra, S. Gélinas, R. H. Friend, *Phys. Rev. B* **2012**, *85*, 045209; c) V. Jankus, E. W. Snedden, D. W. Bright, V. L. Whittle, J. Williams, A. Monkman, *Adv. Funct. Mater.* **2013**, *23*, 384; d) V. Jankus, C. J. Chiang, F. Dias, A. P. Monkman, *Adv. Mater.* **2013**, *25*, 1455; e) Y. Luo, H. Aziz, *Adv. Funct. Mater.* **2010**, *20*, 1285; f) R. Johnson, R. Merrifield, P. Avakian, R. Flippen, *Phys. Rev. Lett.* **1967**, *19*, 285; g) R. Merrifield, *Pure Appl. Chem.* **1971**, *27*, 481.

[6] a) A. Endo, M. Ogasawara, A. Takahashi, D. Yokoyama, Y. Kato, C. Adachi, *Adv. Mater.* **2009**, *21*, 4802; b) H. Uoyama, K. Goushi, K. Shizu, H. Nomura, C. Adachi, *Nature* **2012**, *492*, 234; c) Q. Zhang, B. Li, S. Huang, H. Nomura, H. Tanaka, C. Adachi,

Nat. Photonics **2014**, *8*, 326; d) J. C. Deaton, S. C. Switalski, D. Y. Kondakov, R. H. Young, T. D. Pawlik, D. J. Giesen, S. B. Harkins, A. J. Miller, S. F. Mickenberg, J. C. Peters, *J. Am. Chem. Soc.* **2010**, *132*, 9499; e) Y. Yuan, J.-X. Chen, F. Lu, Q.-X. Tong, Q.-D. Yang, H.-W. Mo, T.-W. Ng, F.-L. Wong, Z.-Q. Guo, J. Ye, *Chem. Mater.* **2013**, *25*, 4957.

[7] Q. Peng, A. Obolda, M. Zhang, F. Li, *Angew. Chem. Int. Ed.* **2015**, *54*, 7091.

[8] a) D. Velasco, S. Castellanos, M. López, F. López-Calahorra, E. Brillas, L. Juliá, *J. Org. Chem.* **2007**, *72*, 7523; b) A. Heckmann, C. Lambert, M. Goebel, R. Wortmann, *Angew. Chem. Int. Ed.* **2004**, *43*, 5851; c) Y. Hattori, T. Kusamoto, H. Nishihara, *Angew. Chem. Int. Ed.* **2014**, *53*, 11845.

[9] a) J. Ye, Z. Chen, M.-K. Fung, C. Zheng, X. Ou, X. Zhang, Y. Yuan, C.-S. Lee, *Chem. Mater.* **2013**, *25*, 2630; b) S. Tang, M. Liu, P. Lu, H. Xia, M. Li, Z. Xie, F. Shen, C. Gu, H. Wang, B. Yang, *Adv. Funct. Mater.* **2007**, *17*, 2869; c) Z. Gao, Y. Liu, Z. Wang, F. Shen, H. Liu, G. Sun, L. Yao, Y. Lv, P. Lu, Y. Ma, *Chem. -Eur. J.* **2013**, *19*, 2602; d) C. C. Wu, Y. T. Lin, K. T. Wong, R.-T. Chen, Y.-Y. Chien, *Adv. Mater.* **2004**, *16*, 61; e) J. Y. Hu, Y. J. Pu, F. Satoh, S. Kawata, H. Katagiri, H. Sasabe, J. Kido, *Adv. Funct. Mater.* **2014**, *24*, 2064.

[10] M. J. Frisch, G. W. Trucks, H. B. Schlegel, G. E. Scuseria, M. A. Robb, J. R. Cheeseman, G. Scalmani, V. Barone, B. Mennucci, G. A. Petersson, H. Nakatsuji, M. Caricato, X. Li, H. P. Hratchian, A. F. Izmaylov, J. Bloino, G. Zheng, J. L. Sonnenberg, M. Hada, M. Ehara, K. Toyota, R. Fukuda, J. Hasegawa, M. Ishida, T. Nakajima, Y. Honda, O. Kitao, H. Nakai, T. Vreven, J. A. Montgomery Jr., J. E. Peralta, F. Ogliaro, M. Bearpark, J. J. Heyd, E. Brothers, K. N. Kudin, V. N. Staroverov, R. Kobayashi, J. Normand, K. Raghavachari, A. Rendell, J. C. Burant, S. S. Iyengar, J. Tomasi, M. Cossi, N. Rega, J. M. Millam, M. Klene, J. E. Knox, J. B. Cross, V. Bakken, C. Adamo, J. Jaramillo, R. Gomperts, R. E. Stratmann, O. Yazyev, A. J. Austin, R. Cammi, C. Pomelli, J. W. Ochterski, R. L. Martin, K. Morokuma, V. G. Zakrzewski, G. A. Voth, P. Salvador, J. J. Dannenberg, S. Dapprich, A. D. Daniels, Ö. Farkas, J. B. Foresman, J. V. Ortiz, J. Cioslowski, D. J. Fox, *Gaussian 09, Revision D.01*, Gaussian, Inc. Wallingford, CT **2009**.

[11] a) W. Li, Y. Pan, R. Xiao, Q. Peng, S. Zhang, D. Ma, F. Li, F. Shen, Y. Wang, B. Yang, *Adv. Funct. Mater.* **2014**, *24*, 1609; b) Y. Pan, W. Li, S. Zhang, L. Yao, C. Gu, H. Xu, B. Yang, Y. Ma, *Adv. Opt. Mater.* **2014**, *2*, 510; c) L. Yao, S. Zhang, R. Wang, W. Li, F. Shen, B. Yang, Y. Ma, *Angew. Chem.* **2014**, *126*, 2151.

[12] a) Y. Cao, I. D. Parker, G. Yu, C. Zhang, A. J. Heeger, *Nature* **1999**, *397*, 414; b) Z. Shuai, D. Beljonne, R. Silbey, J.-L. Brédas, *Phys. Rev. Lett.* **2000**, *84*, 131; c) M. Wohlgenannt, K. Tandon, S. Mazumdar, S. Ramasesha, Z. V. Vardeny, *Nature* **2001**, *409*, 494; d) C. G. Zhen, Y. F. Dai, W. J. Zeng, Z. Ma, Z. K. Chen, J. Kieffer, *Adv. Funct. Mater.* **2011**, *21*, 699.

[13] a) V. Ern, R. E. Merrifield, *Phys. Rev. Lett.* **1968**, *21*, 609; b) P. Desai, P. Shakya, T. Kreouzis, W. P. Gillin, *Phys. Rev. B* **2007**, *75*, 094423; c) Y. Meng, X. Liu, B. Di, Z. An, *J. Chem. Phys.* **2009**, *131*, 244502; d) J. Y. Song, N. Stingelin, A. J. Drew, T. Kreouzis, W. P. Gillin, *Phys. Rev. B* **2010**, *82*, 085205; e) T. L. Keevers, W. J. Baker, D. R. McCamey, *Phys. Rev. B* **2015**, *91*, 205206.

[14] J. Kalinowski, M. Cocchi, D. Virgili, P. Di Marco, V. Fattori, *Chem. Phys. Lett.* **2003**, *380*, 710.

[15] P. Janssen, M. Cox, S. Wouters, M. Kemerink, M. Wienk, B. Koopmans, *Nat. Commun.* **2013**, *4*, 2286.

[16] a) G. Yu, J. Gao, J. C. Hummelen, F. Wudl, A. J. Heeger, *Science* **1995**, *270*, 1789; b) T. Higashino, T. Yamada, M. Yamamoto, A. Furube, N. V. Tkachenko, T. Miura, Y. Kobori, R. Jono, K. Yamashita, H. Imahori, *Angew. Chem. Int. Ed.* **2016**, *55*, 629.

[17] a) C. Li, S. Wang, W. Chen, J. Wei, G. Yang, K. Ye, Y. Liu, Y. Wang, *Chem. Commun.* **2015**, *51*, 10632; b) M. Chen, Y. Yuan, J. Zheng, W. C. Chen, L. J. Shi, Z. L. Zhu, F. Lu, Q. X. Tong, Q. D. Yang, J. Ye, M. Y. Chan, C. S. Lee, *Adv. Optical Mater.* **2015**, *3*, 1215.